Available online at www.sciencedirect.com
ScienceDirect
Nuclear Physics A 00 (2013) 1–8
Nuclear Physics A

Baryon-baryon interactions from chiral effective field theory

J. Haidenbauer

Institute for Advanced Simulation, Institut für Kernphysik (Theorie) and Jülich Center for Hadron Physics, Forschungszentrum Jülich, D-52425 Jülich, Germany

arXiv:1301.1141v1 [nucl-th] 7 Jan 2013

Abstract

Results from an ongoing study of baryon-baryon systems with strangeness $S = -1$ and -2 within chiral effective field theory are reported. The investigations are based on the scheme proposed by Weinberg which has been applied rather successfully to the nucleon-nucleon interaction in the past. Results for the hyperon-nucleon and hyperon-hyperon interactions obtained to leading order are reviewed. Specifically, the issue of extrapolating the binding energy of the H-dibaryon, extracted from recent lattice QCD simulations, to the physical point is addressed. Furthermore, first results for the hyperon-nucleon interaction at next-to-leading order are presented and discussed.

© 2012 Published by Elsevier Ltd.

Keywords: Hyperon-nucleon interaction, Hyperon-hyperon interaction, Lattice QCD, Effective field theory
PACS: 13.75.Ev, 12.39.Fe, 14.20.Pt

1. Introduction

Chiral effective field theory (EFT) as proposed in the pioneering works of Weinberg [1, 2] is a powerful tool for the derivation of nuclear forces. In this scheme there is an underlying power counting which allows to improve calculations systematically by going to higher orders in a perturbative expansion. In addition, it is possible to derive two- and corresponding three-nucleon forces as well as external current operators in a consistent way. Over the last decade or so it has been demonstrated that the nucleon-nucleon (NN) interaction can be described to a high precision within the chiral EFT approach [3, 4]. Following the original suggestion of Weinberg, in these works the power counting is applied to the NN potential rather than to the reaction amplitude. The latter is then obtained from solving a regularized Lippmann-Schwinger equation for the derived interaction potential. The NN potential contains pion-exchanges and a series of contact interactions with an increasing number of derivatives to parameterize the shorter ranged part of the NN force. For reviews we refer the reader to Refs. [5, 6, 7].

In the present contribution I focus on recent investigations by the groups in Bonn-Jülich and Munich on the baryon-baryon interaction involving strange baryons, performed within chiral EFT [8, 9, 10, 11, 12]. In these works the same scheme as applied in Ref. [4] to the NN interaction is adopted. First I discuss the application to the strangeness $S = -1$ sector (ΛN, ΣN). Here the extension of our study [8] to next-to-leading order (NLO) is in progress [12] and a first glimpse on the (still preliminary) achieved results for the ΛN and ΣN interactions will be given. Then I report results of a study on the strangeness $S = -2$ sector, i.e. for the $\Lambda\Lambda$, $\Sigma\Sigma$, and cascade-nucleon (ΞN) interactions. Predictions obtained at leading order (LO) [9] are reviewed and implications for the H-dibaryon are discussed, based on our framework, in the light of recent lattice QCD calculations where evidence for the existence of such a state was found.

At LO in the power counting, as considered in the aforementioned investigations [8, 9, 10], the baryon-baryon potentials involving strange baryons consist of four-baryon contact terms without derivatives and of one-pseudoscalar-meson exchanges, analogous to the NN potential of [4]. The potentials are derived using constraints from SU(3) flavor symmetry. At NLO one gets contributions from two-pseudoscalar-meson exchange diagrams and from four-baryon contact terms with two derivatives [4].

The paper is structured as follows: In Sect. 2 a short overview of the chiral EFT approach is provided. In Sect. 3 results for the ΛN- and ΣN interactions obtained to NLO are presented. In Sect. 4 results for the the $S = -2$ ($\Lambda\Lambda$, ΞN $\Sigma\Sigma$) systems are briefly reviewed and connection is made with lattice QCD results for the H-dibaryon case. The paper ends with a short Summary.

2. Formalism

The derivation of the chiral baryon-baryon potentials for the strangeness sector at LO using the Weinberg power counting is outlined in Refs. [8, 10, 14]. Details for the NLO case will be presented in a forthcoming paper [12], see also [11, 13]. The LO potential consists of four-baryon contact terms without derivatives and of one-pseudoscalar-meson exchanges while at NLO contact terms with two derivatives arise, together with contributions from (irreducible) two-pseudoscalar-meson exchanges.

The spin- and momentum structure of the potentials resulting from the contact terms to LO is given by

$$V^{(0)}_{BB\to BB} = C_{S;\,BB\to BB} + C_{T;\,BB\to BB}(\boldsymbol{\sigma}_1\cdot\boldsymbol{\sigma}_2) \tag{1}$$

in the notation of [4] where the $C_{i;\,BB\to BB}$'s are so-called low-energy coefficients (LECs) that need to be determined by a fit to data. Due to the imposed $\mathrm{SU(3)_f}$ constraints there are only five independent LECs for the NN and the YN sectors together, as described in Ref. [8] where also the relations between the various $C_{i;\,BB\to BB}$'s are given. A sixth LEC is, however, present in the strangeness $S = -2$ channels with isospin $I = 0$.

In next-to-leading order one gets the following spin- and momentum structure:

$$\begin{aligned} V^{(2)}_{BB\to BB} &= C_1\mathbf{q}^2 + C_2\mathbf{k}^2 + (C_3\mathbf{q}^2 + C_4\mathbf{k}^2)(\boldsymbol{\sigma}_1\cdot\boldsymbol{\sigma}_2) + iC_5(\boldsymbol{\sigma}_1+\boldsymbol{\sigma}_2)\cdot(\mathbf{q}\times\mathbf{k}) \\ &+ C_6(\mathbf{q}\cdot\boldsymbol{\sigma}_1)(\mathbf{q}\cdot\boldsymbol{\sigma}_2) + C_7(\mathbf{k}\cdot\boldsymbol{\sigma}_1)(\mathbf{k}\cdot\boldsymbol{\sigma}_2) + iC_8(\boldsymbol{\sigma}_1-\boldsymbol{\sigma}_2)\cdot(\mathbf{q}\times\mathbf{k}). \end{aligned} \tag{2}$$

The transferred and average momentum, $\mathbf{q}$ and $\mathbf{k}$, are defined in terms of the final and initial center-of-mass (c.m.) momenta of the baryons, $\mathbf{p}'$ and $\mathbf{p}$, as $\mathbf{q} = \mathbf{p}' - \mathbf{p}$ and $\mathbf{k} = (\mathbf{p}' + \mathbf{p})/2$. The C_i's (actually $C_{i;\,BB\to BB}$'s) are additional LECs. Performing a partial wave projection and imposing again $\mathrm{SU(3)_f}$ symmetry one finds that in case of the YN interaction there are eight new LECs entering the S-waves and S-D transitions, respectively, and ten coefficents in the P-waves. There are further (four) LECs that contribute only to the $S = -2$ system.

The spin-space part of the one-pseudoscalar-meson-exchange potential is similar to the static one-pion-exchange potential (recoil and relativistic corrections give higher order contributions) and follows from the $\mathrm{SU(3)_f}$ invariant pseudoscalar-meson–baryon interaction Lagrangian with the appropriate symmetries as discussed in [8]:

$$V^{OBE} = -f_{B_1B_1'P}\,f_{B_2B_2'P}\,\frac{(\boldsymbol{\sigma}_1\cdot\mathbf{q})\,(\boldsymbol{\sigma}_2\cdot\mathbf{q})}{\mathbf{q}^2 + M_P^2}\ . \tag{3}$$

Here, M_P is the mass of the exchanged pseudoscalar meson. The coupling constants $f_{BB'P}$ at the various baryon-baryon-meson vertices are fixed by the imposed SU(3) constraints and tabulated, e.g., in [8]. They can be expressed in terms of $f \equiv g_A/2F_\pi \equiv f_{NN\pi}$ ($g_A = 1.26$, $F_\pi = 92.4$ MeV) and α, the so-called $F/(F+D)$-ratio, for which we adopted the SU(6) value ($\alpha = 0.4$). Note that we use the physical masses of the exchanged pseudoscalar mesons. Thus, the explicit SU(3) breaking reflected in the mass splitting between the pseudoscalar mesons is taken into account. The η meson was identified with the octet η (η_8) and its physical mass was used. The two-pseudoscalar-meson-exchange potential can be found in Refs. [11, 12].

The reaction amplitudes are obtained from the solution of a coupled-channels Lippmann-Schwinger (LS) equation for the interaction potentials:

$$T^{\nu''\nu',J}_{\rho''\rho'}(p'',p';\,\sqrt{s}) = V^{\nu''\nu',J}_{\rho''\rho'}(p'',p') + \sum_{\rho,\nu}\int_0^\infty \frac{dpp^2}{(2\pi)^3}\,V^{\nu''\nu,J}_{\rho''\rho}(p'',p)\frac{2\mu_\nu}{q_\nu^2 - p^2 + i\eta}T^{\nu\nu',J}_{\rho\rho'}(p,p';\,\sqrt{s})\,. \tag{4}$$

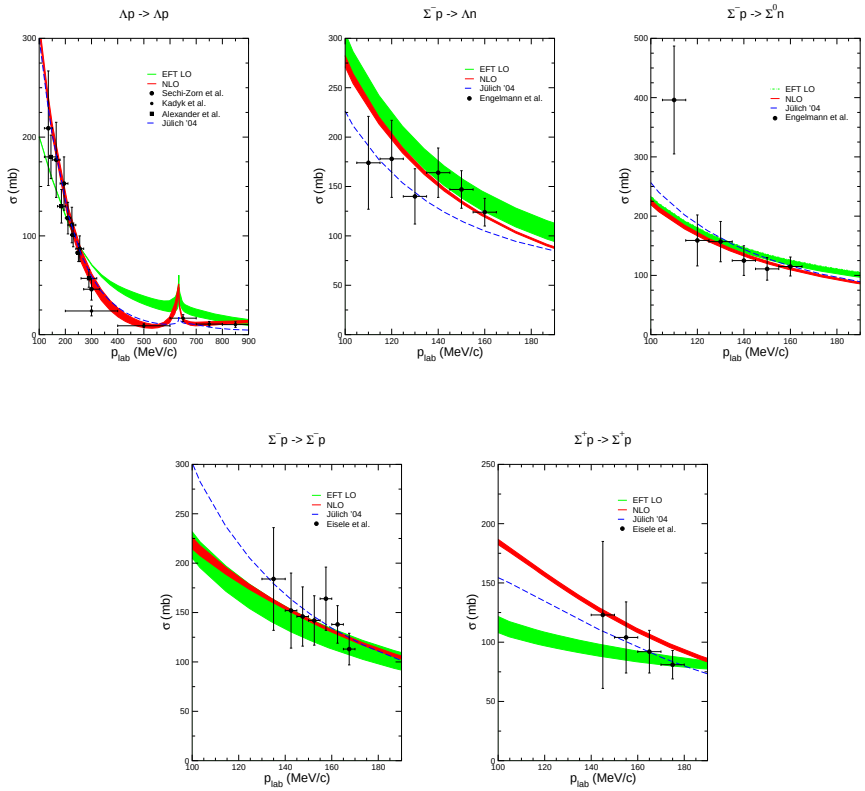


Figure 1. Total cross sections for $\Lambda p \to \Lambda p$, $\Sigma^- p \to \Lambda n$, $\Sigma^- p \to \Sigma^0 n$, $\Sigma^- p \to \Sigma^- p$ and $\Sigma^+ p \to \Sigma^+ p$ as a function of p_{lab}. The green (grey) band shows the chiral EFT results to LO for variations of the cut-off in the range $\Lambda = 550...700$ MeV, while the red (black) band are results to NLO for $\Lambda = 500...700$ MeV. The dashed curve is the result of the Jülich '04 [16] meson-exchange potential.

The label ν indicates the particle channels and the label ρ the partial wave. μ_ν is the pertinent reduced mass. The on-shell momentum in the intermediate state, q_ν, is defined by $\sqrt{s} = \sqrt{m_{B_{1,\nu}}^2 + q_\nu^2} + \sqrt{m_{B_{2,\nu}}^2 + q_\nu^2}$. Relativistic kinematics is used for relating the laboratory energy $T_{\rm lab}$ of the hyperons to the c.m. momentum.

We solve the LS equation in the particle basis, in order to incorporate the correct physical thresholds. Depending on the specific values of strangeness and charge up to six baryon-baryon channels can couple. For the $S = -1$ sector where a comparison with scattering data is possible the Coulomb interaction is taken into account appropriately via the Vincent-Phatak method [15]. The potentials in the LS equation are cut off with a regulator function, $\exp\left[-\left(p'^4 + p^4\right)/\Lambda^4\right]$, in order to remove high-energy components of the baryon and pseudoscalar meson fields [4]. We consider cut-off values in the range 500, ..., 700 MeV, similar to what was used for chiral NN potentials [4].

3. Results for the strangeness S=-1 sector

The imposed SU(3) flavor symmetry implies that at LO five independent LECs contribute to the YN interaction [8]. These five contact terms were determined in [8] by a fit to the YN scattering data. Already in that scenario a fairly reasonable description of the 35 low-energy YN scattering data could be achieved for cutoff values $\Lambda = 550, ..., 700$ MeV and for natural values of the LECs. At NLO there are eight new contact terms contributing to the S-waves and the $^3S_1$-$^3D_1$ transition, and ten in the P-waves. Once again the corresponding LECs were fixed by fitting to the data. The results obtained at NLO are presented in Fig. 1 (black (red) bands), together with those at LO (grey (green) bands).

The bands represent the variation of the cross sections based on chiral EFT within the considered cutoff region. For comparison also results for the Jülich '04 [16] meson-exchange models are shown (dashed line).

Obviously, and as expected, the energy dependence exhibited by the data can be significantly better reproduced within our NLO calculation. This concerns in particular the $\Sigma^+ p$ channel. But also for Λp the NLO results are now well in line with the data even up to the ΣN threshold. Furthermore, one can see that the dependence on the cutoff mass is strongly reduced in the NLO case.

Note that in case of LO as well as at NLO no $SU(3)_f$ constraints from the NN sector were imposed in the fitting procedure. The leading order $SU(3)_f$ breaking in the one-boson exchange diagrams (coupling constants) is ignored.

Besides an excellent description of the YN data the chiral EFT interaction also yields a correctly bound hypertriton, see Table 1. Indeed this binding energy had to be included in the fitting procedure because otherwise it would have not been possible to fix the relative strength of the (S-wave) singlet- and triplet contributions to the Λp interaction. Table 1 lists also results for two meson-exchange potentials, namely of the Jülich '04 model [16] and the Nijmegen NSC97f potential [17], which both reproduce the hypertriton binding energy correctly. Obviously, the scattering lengths predicted at NLO are larger than those obtained at LO and now similar to the values of the meson-exchange potentials. The $\Sigma^+ p$ scattering length in the $^3S_1$ partial wave is positive, as it was already the case for our LO potential, indicating a repulsive interaction in this channel.

	EFT LO	EFT NLO	Jülich '04 [16]	NSC97f [17]	experiment
Λ [MeV]	$550 \cdots 700$	$500 \cdots 700$			
$a_s^{\Lambda p}$	$-1.90 \cdots -1.91$	$-2.88 \cdots -2.89$	-2.56	-2.51	$-1.8^{+2.3}_{-4.2}$
$a_t^{\Lambda p}$	$-1.22 \cdots -1.23$	$-1.59 \cdots -1.61$	-1.66	-1.75	$-1.6^{+1.1}_{-0.8}$
$a_s^{\Sigma^+ p}$	$-2.24 \cdots -2.36$	$-3.90 \cdots -3.83$	-4.71	-4.35	
$a_t^{\Sigma^+ p}$	$0.70 \cdots 0.60$	$0.51 \cdots 0.47$	0.29	-0.25	
$(^3_\Lambda\mathrm{H})$ E_B	$-2.34 \cdots -2.36$	$-2.31 \cdots -2.34$	-2.27	-2.30	-2.354(50)

Table 1. The YN singlet (s) and triplet (t) scattering lengths (in fm) and the hypertriton binding energy, E_B (in MeV).

Calculations for the four-body hypernuclei $^4_\Lambda$H and $^4_\Lambda$He based on those interactions are reported in Ref. [18].

4. Results for the strangeness $S = -2$ sector

In this section I review results obtained for the $S = -2$ sector, specifically for the coupled $\Lambda\Lambda - \Xi N - \Sigma\Sigma$ system, within chiral EFT at LO [9, 19, 20]. As mentioned above, at LO one additional LEC occurs in this specific channel with $I = 0$ which, in principle, should be determined from experimental information available for this sector. However, the scarce data ($\Xi^- p \to \Xi^- p$ and $\Xi^- p \to \Lambda\Lambda$ cross sections [21]) are afflicted with large uncertainties and, thus, do not allow to establish reliably its value as found by us [9]. Some results for strangeness $S = -2$ published in [9] are reproduced here in Fig. 2. As before the band reflects the dependence of the results on variations of the cutoff Λ. The cutoff was varied between 550 and 700 MeV (like in case of the LO YN potential) and under the constraint that the $\Lambda\Lambda$ $^1S_0$ scattering length remains practically unchanged [9]. As reference we have taken the result for $\Lambda = 600$ MeV and with the value of the additional LEC fixed in such a way that $C_{\Lambda\Lambda\to\Lambda\Lambda} = 0$. The scattering length turned out to be $a_s^{\Lambda\Lambda} = -1.52$ fm [9]. Analyses of the measured binding energy of the double-strange hypernucleus $^{\ 6}_{\Lambda\Lambda}$He [22] suggest that the $\Lambda\Lambda$ scattering length could be in the range of -1.3 to -0.7 fm [23, 24, 25]. A first determination of the scattering length utilizing data on the $\Lambda\Lambda$ invariant mass from the reaction $^{12}C(K^-, K^+\Lambda\Lambda X)$ [26] led to the result $a_s^{\Lambda\Lambda} = -1.2 \pm 0.6$ fm [27].

One particular interesting aspect of the coupled $\Lambda\Lambda - \Xi N - \Sigma\Sigma$ system is the H-dibaryon, a deeply bound 6-quark state with $J = 0$ predicted by Jaffe from the bag model [28], that should occur in this channel. So far none of the experimental searches for the H-dibaryon let to convincing signals [26]. However, recently evidence for a bound H-dibaryon was claimed based on lattice QCD calculations [29, 30, 31, 32]. Extrapolations of those computations, performed for $m_\pi \gtrsim 400$ MeV, to the physical pion mass suggest that the H-dibaryon could be either loosely bound or move into the continuum [33, 34].

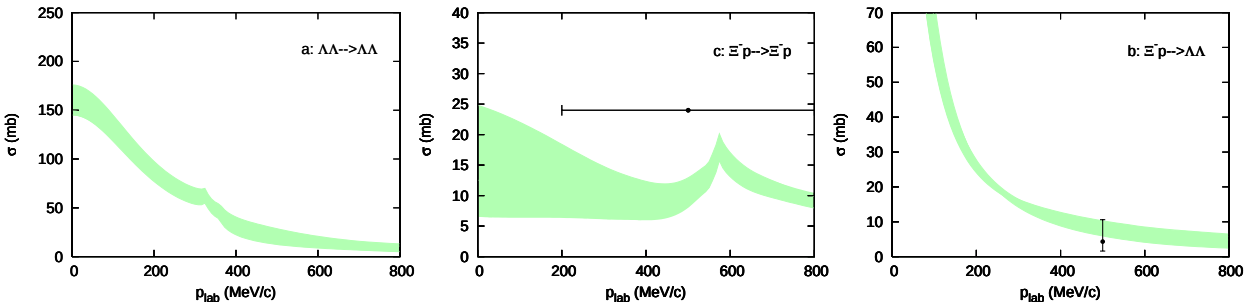


Figure 2. YY and ΞN integrated cross sections as a function of $p_{\rm lab}$. The band shows the chiral EFT result at LO for variations of the cutoff Λ as discussed in the text. Data are from Ref. [21].

Unfortunately, because the mentioned additional contact term cannot be reliably fixed from the data in the $S = -2$ sector, no immediate predictions can be made for the H-dibaryon within chiral EFT. However, the framework can be used as a tool to study the dependence of its conjectured binding energy on the masses of the involved hadrons and, thus, allows for an alternative extrapolation of the results, obtained in lattice QCD calculations at unphysical meson- and baryon masses, down to the physical point. In particular one can fine-tune the "free" LEC to produce a bound H with a given binding energy for meson- and baryon masses corresponding to the lattice simulations, and then study its properties [19, 20] for physical masses. Note that at LO the LECs do not depend on the meson masses (strictly speaking, on the quark masses). Variations of the meson masses enter only in the potential in Eq. (3), those of the baryon masses (via μ_ν) in the LS equation (4).

Let me first consider individual variations of the masses of the involved particles. To begin with I examine the dependence of the H binding energy on the pion mass M_π and keep all other (meson and baryon) masses at their physical value. Corresponding results are displayed in Fig. 3 (left). Adjusting the LEC so that a H binding energy of 13.2 MeV is predicted for $M_\pi = 389$ MeV, corresponding to the result published by NPLQCD [31], yields the dashed curve. The solid curve corresponds to a H-dibaryon that is bound by 1.87 MeV at the physical point, i.e. with the same binding wave number (0.23161 fm^{-1}) as the deuteron in the NN case. Enlarging the pion mass to around 400 MeV for the latter scenario (i.e. to values in an order that corresponds to the NPLQCD calculation [29]) increases the binding energy to around 8 MeV and a further change of M_π to 700 MeV (corresponding roughly to the HAL QCD calculation [30]) yields then 13 MeV.

Note that the dependence on M_π obtained agrees – at least on a qualitative level – with that presented in Ref. [33]. Specifically, our calculation exhibits the same trend (a decrease of the binding energy with decreasing pion mass) and our binding energy of 9 MeV at the physical pion mass is within the error bars of the results given in [33]. On the other hand, we clearly observe a non-linear dependence of the binding energy on the pion mass. As a consequence, scaling our results to the binding energy reported by the HAL QCD Collaboration [30] (30-40 MeV for $M_\pi \approx 700-1000$ MeV) yields binding energies of more than 20 MeV at the physical point, which is certainly outside of the range suggested in Ref. [33]. However, it has to be said that for such large pion masses the LO chiral EFT can not be trusted quantitatively.

Now let me look at the dependence of the H binding energy on the masses of the involved baryons. In case of the H-dibaryon one is dealing with three coupled channels, namely $\Lambda\Lambda$, ΞN, and $\Sigma\Sigma$. Since we know from our experience with coupled-channel problems [8, 10, 16, 35] that coupling effects are sizeable and the actual separation of the various thresholds plays a crucial role, we expect a considerable dependence of the H binding energy on the thresholds (i.e. on the Σ, and on the Ξ and N masses). Corresponding results are displayed in Fig. 3 in the right panel. Note that the pion mass and the masses of the other pseudo-scalar mesons are kept at their physical value while varying the BB thresholds. For the isospin-averaged masses used in the actual calculation the thresholds are at 2231.2, 2257.7, and 2385.0 MeV, respectively. Thus, the physical difference between the $\Lambda\Lambda$ and ΞN thresholds is around 26 MeV while the $\Sigma\Sigma$ threshold is separated from the one for $\Lambda\Lambda$ by roughly 154 MeV.

First I discuss the effect of the $\Sigma\Sigma$ channel because its threshold is quite far from the one of $\Lambda\Lambda$ so that there is a rather drastic breaking of the SU(3) symmetry. Indeed, when the Σ mass is decreased so that the nominal $\Sigma\Sigma$ threshold (at 2385 MeV) moves downwards and finally coincides with the one of the $\Lambda\Lambda$ channel (2231.2 MeV), a concurrent fairly drastic increase in the H binding energy is observed, cf. the solid curve in Fig. 3 for results based on

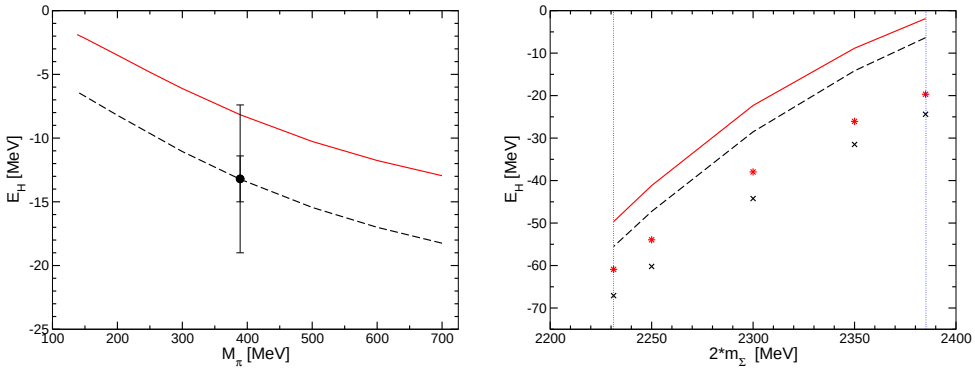


Figure 3. Dependence of the binding energy of a H-dibaryon on the pion mass M_π (left) and on the Σ mass m_Σ (right). The solid curve correspond to the case where the LEC is fixed such that $E_H = -1.87$ MeV for physical masses while for the dashed curve it is fixed to yield $E_H = -13.2$ MeV for $M_\pi = 389$ MeV. The asterisks and crosses represent results where, besides the variation of m_Σ, $m_\Xi + m_N = 2m_\Lambda$ is assumed so that the ΞN threshold coincides with that of the $\Lambda\Lambda$ channel. The vertical (dotted) lines indicate the physical $\Lambda\Lambda$ and $\Sigma\Sigma$ thresholds. The circle indicates the lattice result of the NPLQCD Collaboration [31].

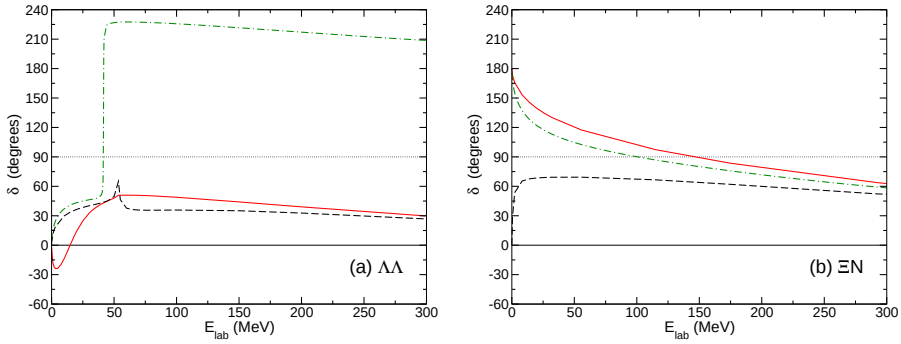


Figure 4. Phase shifts in the $^1S_0$ partial wave in the $I = 0$ channel of $\Lambda\Lambda$ (a) and ΞN (b) as a function of the pertinent laboratory energies. The solid line is the result for our illustrative BB interaction that produces a bound H at $E_H = -1.87$ MeV. The other curves are results for interactions that are fine-tuned to the H binding energies found in the lattice QCD calculations of the HAL QCD (dashed) and NPLQCD (dash-dotted) Collaborations, respectively, for the pertinent meson (pion) and baryon masses as described in the text.

the interaction with a binding energy of 1.87 MeV for physical masses of the mesons and baryons. In this context I want to point out that the direct interaction in the $\Sigma\Sigma$ channel is actually repulsive for the low-energy coefficients fixed from the YN data plus the pseudoscalar meson exchange contributions with coupling constants determined from the SU(3) relations [8], and it remains repulsive even for LEC values that produce a bound H-dibaryon. But the coupling between the channels generates a sizeable effective attraction which increases when the channel thresholds come closer. The dashed curve is a calculation with the contact term fixed to simulate the binding energy (13.2 MeV) of the NPLQCD Collaboration at $M_\pi = 389$ MeV. As one can see, the dependence of the binding energy on the Σ mass is rather similar. The curve is simply shifted downwards by around 4.5 MeV, i.e. by the difference in the binding energy observed already at the physical masses. The asterisks and crosses represent results where, besides the variation of the $\Sigma\Sigma$ threshold, the ΞN threshold is shifted to coincide with that of the $\Lambda\Lambda$ channel. This produces an additional increase of the H binding energy by 20 MeV at the physical $\Sigma\Sigma$ threshold and by 9 MeV for that case where all three BB threshold coincide. Altogether there is an increase in the binding energy of roughly 60 MeV when going from the physical point to the case of baryons with identical masses, i.e. to the SU(3) symmetric situation. This is significantly larger than the variations due to the pion mass considered before.

After these exemplary studies let me now try to connect with the published H binding energies from the lattice QCD calculations [30, 31]. The results obtained by the HAL QCD Collaboration are obviously for the SU(3) symmetric case and the corresponding masses are given in Table I of Ref. [30]. Thus, one can take those masses and then

fix the additional LEC so that their H binding energy is reproduced with those masses. To be concrete: the masses $M_P = 673\,\mathrm{MeV}$ and $m_B = 1485\,\mathrm{MeV}$ are used, and the LEC is fixed so that $E_H = -35\,\mathrm{MeV}$. When now the masses of the baryons and mesons are changed towards their physical values the bound state moves up to the $\Lambda\Lambda$ threshold, crosses the threshold, crosses also the ΞN threshold and then disappears. In fact, qualitatively this outcome can be already read off from the curves in Fig. 3 by combining the effects from the variations in the pion and the baryon masses. Based on those results one expects a shift of the H binding energy in the order of 60 to 70 MeV for the mass parameters of the HAL QCD calculation.

In case of the NPLQCD calculation the values provided in Ref. [36] are taken. Those yield then 17 MeV for the ΞN-$\Lambda\Lambda$ threshold separation (to be compared with the physical value of roughly 26 MeV) and 77 MeV for the $\Sigma\Sigma$-$\Lambda\Lambda$ separation (physical value around 154 MeV). We also use the meson masses of Ref. [36], specifically $M_\pi = 389$ MeV. With those baryon and meson masses again the LEC is fixed so that the H binding energy given by the NPLQCD Collaboration is reproduced, namely $E_H = -13.2$ MeV [31]. Again the masses of the baryons and mesons are changed so that they approach their physical values. Also here the bound state moves up to and crosses the $\Lambda\Lambda$ threshold. However, in the NPLQCD case the state survives and remains below the ΞN threshold at the physical point. Specifically, an unstable bound state [37] is observed in the ΞN system around 5 MeV below its threshold and a corresponding resonance at a kinetic energy of 21 MeV in the $\Lambda\Lambda$ system

Phase shifts for the $\Lambda\Lambda$ and ΞN channels are presented in Fig. 4, for the relevant partial wave ($^1S_0$). The solid line is the result for the BB interaction that produces a loosely bound H-dibaryon with $E_H = -1.87$ MeV. The phase shift for the ΞN channel, Fig. 4 (b), is rather similar to the one for the $^3S_1$ NN partial wave where the deuteron is found, see e.g. [4]. Specifically, it starts at 180°, decreases smoothly and eventually approaches zero (for large energies not shown in the figure). The result for $\Lambda\Lambda$, Fig. 4 (a), behaves rather differently. The pertinent phase commences at zero degrees, is first negative but becomes positive within 20 MeV and finally turns to zero again for large energies. This behaviour of the phase shifts was interpreted in [19] as a signature for that the bound H-dibaryon is actually predominantly a (bound) ΞN state. Indeed, in that work it was argued that it follows already from the assumed (approximate) SU(3) symmetry of the interaction, that any H-dibaryon is very likely a bound ΞN state rather than a $\Lambda\Lambda$ state.

The dashed curve corresponds to the interaction that was fitted to the result of the HAL QCD Collaboration and reproduces their bound H-dibaryon with their meson and baryon masses. The results in Fig. 4 are those obtained with physical masses of the mesons and baryons. The phase shift of the ΞN channel shows no trace of a bound state anymore. Still the phase shift rises up to around 60° near threshold, a behavior quite similar to that of the $^1S_0$ NN partial wave where there is a virtual state (also called antibound state [37]). Indeed, such a virtual state also seems to be present in the ΞN channel as a remnant of the original bound state. The effect of this virtual state can be seen in the $\Lambda\Lambda$ phase shift where it leads to an impressive cusp at the opening of the ΞN channel, cf. the dashed line in Fig. 4 (a).

The ΞN phase shift for the NPLQCD scenario (i.e. for the interaction that reproduces their bound H-dibaryon with their meson and baryon masses), see the dash-dotted curve, starts at 180°, a clear indication for the presence of a bound state. However, in this case the bound state is not located below the $\Lambda\Lambda$ threshold but above, as already mentioned before. Consequently, the corresponding $\Lambda\Lambda$ phase shift exhibits a resonance-like behavior at the energy where the (now quasi) bound H-dibaryon is located.

Phase shifts for the $^1S_0$ $\Sigma\Sigma$ partial wave can be found in Ref. [20]. The predictions of the three considered cases for this channel are practically the same.

5. Summary

Chiral effective field theory, successfully applied in Ref. [4] to the NN interaction, also works well for the baryon-baryon interactions in the strangeness $S = -1$ ($\Lambda N - \Sigma N$) and $S = -2$ ($\Lambda\Lambda - \Xi N - \Sigma\Sigma$) sectors. As shown in our earlier work, already at leading order the bulk properties of the ΛN and ΣN systems can be reasonably well accounted for. The new results for the YN interaction presented here, obtained to next-to-leading order in the Weinberg counting, look very promising. First there is a visible improvement in the quantitative reproduction of the available data on ΛN and ΣN scattering and, secondly, the dependence on the regularization scheme is strongly reduced as compared to the LO result. Indeed the description of the YN system achieved at NLO is now on the same level of quality as the one by the most advanced meson-exchange YN interactions.

The recently reported evidence for the so-called H-dibaryon from lattice QCD calculations stimulated us to investigate also the quark-mass dependence of binding energies for baryon-baryon systems in the strangeness $S = -2$ sector within the chiral EFT framework. Here I presented results of an analysis performed at leading order in the Weinberg counting. We found rather drastic effects caused by the SU(3) breaking related to the values of the three thresholds $\Lambda\Lambda$, $\Sigma\Sigma$ and ΞN. For physical values the binding energy of the H is reduced by as much as 60 MeV as compared to a calculation based on degenerate (i.e. SU(3) symmetric) BB thresholds. Translating this observation to the lattice QCD results reported by the HAL QCD Collaboration [30], we see that the bound state has disappeared at the physical point. For the case of the NPLQCD calculation [31], a resonance in the $\Lambda\Lambda$ system might survive.

6. Acknowledgements

I would like to thank N. Kaiser, U.-G. Meißner, A. Nogga, S. Petschauer, and W. Weise for collaborating on the topic covered by my talk. Work supported in part by DFG and NSFC (CRC 110).

References

[1] S. Weinberg, Phys. Lett. B **251** (1990) 288.
[2] S. Weinberg, Nucl. Phys. B **363** (1991) 3.
[3] D. R. Entem, R. Machleidt, Phys. Rev. C **68** (2003) 041001.
[4] E. Epelbaum, W. Glöckle, U.-G. Meißner, Nucl. Phys. A **747** (2005) 362.
[5] P. F. Bedaque, U. van Kolck, Annu. Rev. Nucl. Part. Sci. **52** (2002) 339.
[6] E. Epelbaum, Prog. Part. Nucl. Phys. **57** (2006) 654.
[7] E. Epelbaum, H. -W. Hammer and U.-G. Meißner, Rev. Mod. Phys. **81** (2009) 1773.
[8] H. Polinder, J. Haidenbauer and U.-G. Meißner, Nucl. Phys. A **779** (2006) 244.
[9] H. Polinder, J. Haidenbauer and U.-G. Meißner, Phys. Lett. B **653** (2007) 29.
[10] J. Haidenbauer, U.-G. Meißner, Phys. Lett. **B684** (2010) 275.
[11] S. Petschauer, diploma thesis, TU Munich, 2011.
[12] J. Haidenbauer et al., in preparation.
[13] S. Petschauer, these proceedings.
[14] J. Haidenbauer, U.-G. Meißner, A. Nogga and H. Polinder, Lect. Notes Phys. **724** (2007) 113.
[15] C.M. Vincent and S.C. Phatak, Phys. Rev. C **10** (1974) 391.
[16] J. Haidenbauer, U.-G. Meißner, Phys. Rev. C **72** (2005) 044005.
[17] T. A. Rijken, V. G. J. Stoks, Y. Yamamoto, Phys. Rev. C **59** (1999) 21.
[18] A. Nogga, these proceedings.
[19] J. Haidenbauer, U.-G. Meißner, Phys. Lett. B **706** (2011) 100.
[20] J. Haidenbauer and U.-G. Meißner, Nucl. Phys. A **881** (2012) 44.
[21] J. K. Ahn *et al.*, Phys. Lett. B **633** (2006) 214.
[22] H. Takahashi *et al.*, Phys. Rev. Lett. **87** (2001) 212502.
[23] I. N. Filikhin, A. Gal, V. M. Suslov, Phys. Rev. C **68** (2003) 024002.
[24] T. A. Rijken, Y. Yamamoto, Phys. Rev. C **73** (2006) 044008.
[25] Y. Fujiwara, Y. Suzuki, C. Nakamoto, Prog. Part. Nucl. Phys. **58** (2007) 439.
[26] C.J. Yoon *et al.*, Phys. Rev. C **75** (2007) 022201.
[27] A.M. Gasparyan, J. Haidenbauer, C. Hanhart, Phys. Rev. C **85** (2012) 015204.
[28] R. L. Jaffe, Phys. Rev. Lett. **38** (1977) 195 [Erratum-ibid. **38** (1977) 617].
[29] S. R. Beane *et al.*, Phys. Rev. Lett. **106** (2011) 162001.
[30] T. Inoue *et al.*,, Phys. Rev. Lett. **106** (2011) 162002.
[31] S. R. Beane *et al.*, Phys. Rev. D **85** (2012) 054511.
[32] T. Inoue *et al.*, Nucl. Phys. A **881** (2012) 28.
[33] S. R. Beane *et al.*, Mod. Phys. Lett. A **26** (2011) 2587.
[34] P. E. Shanahan, A. W. Thomas, R. D. Young, Phys. Rev. Lett. **107** (2011) 092004.
[35] J. Haidenbauer, G. Krein, U.-G. Meißner, L. Tolos, Eur. Phys. J. A **47** (2011) 18.
[36] S. R. Beane et al., Phys. Rev. D **84** (2011) 014507.
[37] A. M. Badalyan, L. P. Kok, M. I. Polikarpov, Yu. A. Simonov, Phys. Rept. **82** (1982) 31.